sciendo

Ekológia (Bratislava) - Journal of the Institute of Landscape Ecology, Slovak Academy of Sciences Vol. 44, No. 2, p. 205–211, 2025

DOI:10.2478/eko-2025-0023

INSIGHTS FROM COMPARATIVE ANALYSIS OF RADAR AND OPTICAL VEGETATION INDICES: A CASE STUDY IN GILAN PROVINCE, IRAN

BEHNAM ASGHARI BEIRAMI[1], SEYED OMID REZA SHOBAIRI ✉[2]

[1]Imam Hossein University, Tehran, Iran
[2]Xinjiang Institute of Ecology and Geography, Chinese Academy of Sciences, Urumqi, 830011, China; e-mail: omidshobeyri214@gmail.com

✉ Corresponding author

Received: 5 April 2025 / **Accepted:** 30 July 2025

Abstract

Beirami B.A., Shobairi S.O.R.: Insights from comparative analysis of radar and optical vegetation indices: a case study in Gilan province, Iran[†]. Ekológia (Bratislava), Vol. 44, No. 2, p. 205–211, 2025.

This study evaluates the relationships between Sentinel-1 radar vegetation indices (modified radar vegetation index [mRVI], modified Radar Forest Degradation Index [mRFDI]) and Sentinel-2 optical indices (normalized differential vegetation index [NDVI], ratio vegetation index [RVI]) across diverse land covers in Gilan province, Iran—a region characterized by humid subtropical climates, frequent cloud cover, and threatened ecosystems. Using Google Earth Engine, we analyzed summer 2023 data, comparing indices in non-vegetated, sparse, dense, and mixed landscapes. Results revealed near-perfect inverse correlations between radar indices (mRVI–mRFDI: $r \approx -0.99$) across all environments, confirming their structural consistency. Radar–optical correlations, however, were landcover dependent: negligible in non-vegetated ($|r| < 0.15$) and dense-vegetated ($|r| < 0.05$), but moderate in mixed zones (e.g., mRVI–NDVI: $r = 0.42$) where structural (radar) and biochemical (optical) signals partially aligned. Sparse vegetation showed transitional ties (mRVI–RVI: $r = 0.39$), highlighting early sensor synergy. Radar excelled in detecting degradation and soil moisture under cloud cover, while optical indices tracked chlorophyll dynamics but faltered in dense canopies. These findings underscore the complementary roles of Synthetic Aperture Radar and optical sensors: integrated use is critical in homogeneous areas (e.g., forests), while mixed landscapes benefit from inherent synergies, reducing reliance on resource-intensive fusion. This study advances tailored multi-sensor strategies for cloud-prone regions, enhancing vegetation monitoring accuracy to support sustainable management in ecologically sensitive zones like Gilan.

Key words: Sentinel, vegetation index, NDVI, SAR, remote sensing, Gilan province.

Introduction

Nowadays, remote sensing images have become a simple and efficient tool for ecological and environmental studies due to their cheapness and wide geographic coverage. In general, remote sensing sensors are divided into two groups: active and passive sensors (Zhou et al., 2021).

Passive sensors, such as the European Space Agency's Sentinel-2, use the sun as an energy source and record the reflected light from the Earth's surface features. This recorded light intensity is represented as grayscale pixels, which, after various corrections, are converted into useful information using image processing and statistical methods. Algebraic image processing methods such as the normalized differential vegetation index (NDVI) or the ratio vegetation index (RVI) have a special place in studying vegetation (Xue, Su, 2017). However, optical remote sensing is limited by cloud cover, atmospheric interference, and lighting conditions, which often hinder consistent data acquisition.

On the other hand, active Synthetic Aperture Radar (SAR) sensors such as Sentinel-1 provide their own source of energy and then record the backscatter radiation of surface classes. Unlike optical sensors such as Sentinel-2, which take into account the spectral behavior of features, the SAR backscatter coefficient is affected by the structure, roughness, dielectric constant, humidity, and other characteristics of the ground features (Shao et al., 2003). In addition, unlike optical sensors that have limitations in imaging at night and where the presence of clouds affects the obtained images, SAR images are capable of capturing images at all times and in all weather conditions (Tsokas et al., 2022). In recent years, various efforts have been made to develop indices for extracting vegetation characteristics from SAR images, of which the modified Radar Vegetation Index (mRVI) and modified Radar Forest Degradation Index (mRFDI) indices are among the most prominent (Çolak et al., 2021; Nicolau et al., 2021). Due to the different nature of these indices compared to optical indices, various studies have been conducted to compare these two groups of vegetation indices. The following are some of the most important studies that use the optical vegetation indices (OVIs) and radar vegetation indices (RVIs) to study the vegetation.

Gupta's study compares the sensitivity of RVI and NDVI for agricultural monitoring and shows that RVI is more sensitive during early wheat growth stages (Gupta, 1993). Spadoni et al's study aims to produce high-resolution forest raster cartography for Italy using Sentinel-2 multispectral images and NDVI to differentiate vegetation types. By analyzing NDVI trends, this research improves classification accuracy, particularly in distinguishing arboreal from non-arboreal vegetation, and generates accurate and updatable forest maps (Spadoni et al., 2020). De La Iglesia Martinez and Labib (2023)'s study analyzes the sensitivity of NDVI to different vegetation types and amounts within urban areas and shows that NDVI changes follow nonlinear trends and are more influenced by canopy and shrub coverage than grass. The findings highlight the need for careful evaluation of NDVI in urban greening policies to accurately interpret vegetation changes and their impact on health and the environment. Shobairi et al (2024)'s study analyzed satellite data in the Tian Shan ecoregions from 2000 to 2022 and showed that NDVI outperformed EVI in tracking vegetation expansion, which was influenced more by human activities than climate factors. A comparative study on the OVIs was performed by Xue and Su (2017).

Yong-Hyun et al's study compares RVI from RADARSAT-2 with multispectral vegetation indices (NDVI and SAVI) from Landsat-8 across different land covers (Kim et al., 2014). The results show similar patterns, suggesting that RVI can be a reliable alternative to multispectral vegetation indices for vegetation analysis, especially in low-visibility conditions like bad weather or nighttime. The study of Gonenc and Ozerdem (2019) compared the RVI from RADARSAT-2 and NDVI from Landsat-8 over agricultural areas using 100 GPS points. The results showed a strong correlation (about 50%) between RVI and NDVI, suggesting that RVI can be effectively used as an alternative vegetation index under various conditions. Çolak et al (2021)'s study used Sentinel-1 SAR and Sentinel-2 optical time series data in Google Earth Engine (GEE) to analyze land cover changes due to the construction of the Sinop Nuclear Power Plant in Turkey from 2015 to 2020. The results showed significant deforestation, with strong negative correlations (−0.99) between RVIs and reported land cover loss, confirming substantial environmental impact. Wu et al (2025)'s study examines the correlation between OVIs (NDVI, EVI, DVI) and radar parameters and the RVI using Sentinel-1A and Sentinel-2A imagery at the plot level. Results show that VH backscatter consistently has the strongest correlation with optical indices, while patch size and landscape shape index significantly influence these relationships, providing insights for improving remote sensing-based agricultural monitoring. A comparative study on the RVIs can be found in Hu et al. (2024).

As can be seen from the literature review, both OVIs and RVIs are used in the different studies for simply investigating the situation of the vegetation land covers, but the relationship between them is still an open question for different landcovers in different geographic and climate situations. This study aims to systematically evaluate the correlation between Sentinel-1 and Sentinel-2 vegetation indices across varying vegetation densities in Gilan province in the north of Iran. By evaluating both Sentinel-1 (mRFDI, mRVI) and Sentinel-2 (NDVI, RVI) indices, this research contributes to better insights into the use of OVIs and RVIs for vegetation monitoring in areas with frequent cloud cover, such as north of Iran.

Study area and data

Gilan province (Fig. 1), located in northern Iran (37°26´N 49°33´E), features a humid subtropical climate with high rainfall (1,200–1,800 mm/year) and diverse landscapes, including the UNESCO-listed Hyrcanian forests, fertile lowland rice paddies, tea plantations, and the Anzali Lagoon wetlands. Bordered by the Caspian Sea and Alborz Mountains, its elevation ranges from coastal plains to 3,000-m peaks, supporting rich biodiversity and agriculture (e.g., citrus, sericulture). However, urbanization, deforestation, and climate pressures threaten its ecosystems, making it a critical region for remote sensing studies on land-use change, wetland degradation, and sustainable management. Gilan's land cover and ecological diversity make it ideal for com-

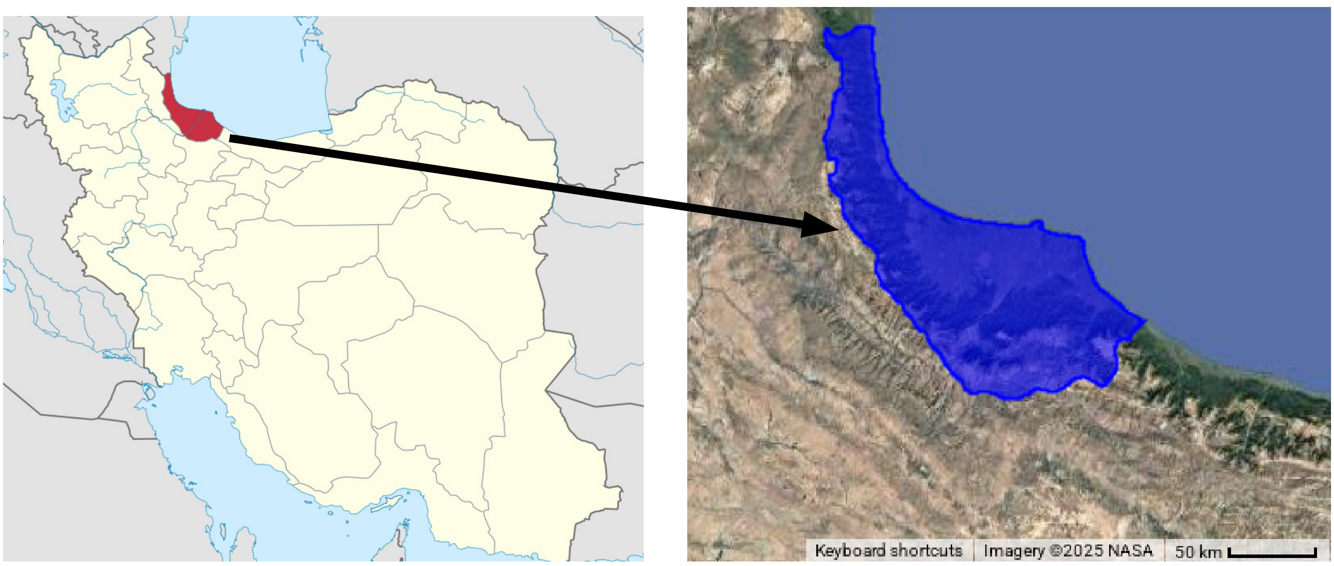

Fig. 1. Gilan province in Iran.

paring radar (e.g., Sentinel-1) and optical (e.g., Sentinel-2) vegetation indices. Radar's all-weather capability overcomes cloud obstruction, while optical sensors provide spectral detail for chlorophyll dynamics. Comparing RVIs and OVIs in Gilan provides valuable insights into vegetation behavior in two different ranges of the electromagnetic spectrum that can help with sustainable land management, which is essential for preserving environmentally sensitive forests, wetlands, and agricultural lands.

This study focuses on using Sentinel-1 and Sentinel-2 satellite data in GEE from 2023-07-06 to 2023-09-06 to analyze the relationships between OVIs and RVIs in Gilan Province. The datasets used in this study include the following:

- **Sentinel-1 SAR data:** The Sentinel-1 mission provides C-band SAR data at 5.405 GHz, including Ground Range Detected scenes that are processed with the Sentinel-1 Toolbox for calibration and ortho-correction. Updated daily, the collection includes scenes at 10, 25, or 40-m resolutions with four polarization combinations (VV, HH, VV + VH, and HH + HV) and an additional incidence angle band. Preprocessing steps involve thermal noise removal, radiometric calibration, and terrain correction using SRTM 30 or ASTER DEM, with final values converted to decibels. This dataset is used to compute the RVIs in this study for assessing vegetation behaviors in the microwave (or radio) domain of the electromagnetic spectrum.
- **Sentinel-2 optical data:** Sentinel-2 is a high-resolution, multi-spectral satellite mission designed for land monitoring, including vegetation, water, and soil observation. Its Level-2 data provides surface reflectance imagery with 12 spectral bands. After January 2022, newer Sentinel-2 scenes underwent a DN value adjustment, which was later harmonized to maintain consistency with older data. The QA60 band, used for cloud detection, was updated in 2024 to use improved cloud classification methods. While Sentinel-2 offers global coverage, some earlier data may have gaps. This dataset is used to compute OVIs in this study for assessing vegetation behaviors in the optical domain of the electromagnetic spectrum.

Methodology

This study follows a structured methodology to ensure an accurate and comprehensive comparison between RVIs and OVIs. The proposed methodology's simplified flowchart is shown in Fig. 2. The main steps of the study are as follows:

1. **Data preprocessing:**
   - **Sentinel-1 preprocessing:** As mentioned earlier, many of the important preprocessing steps are done by GEE, and we only convert the values of DN to gamma backscattering coefficients. Due to better using of resources, we also downscale the pixel size to 50 m. In addition, we use the composite mean value of each pixel in the time period to generate the final SAR image.
   - **Sentinel-2 preprocessing:** As mentioned earlier, many of the important preprocessing steps are done by GEE. After cloud filtering, Sentinel-2 reflectance data area used in experiments. Due to better using of resources, we also downscale the pixel size to 50 m. In addition, similar to SAR data, we use the composite mean value of each pixel in the time period to generate the final Sentinel-2 image.

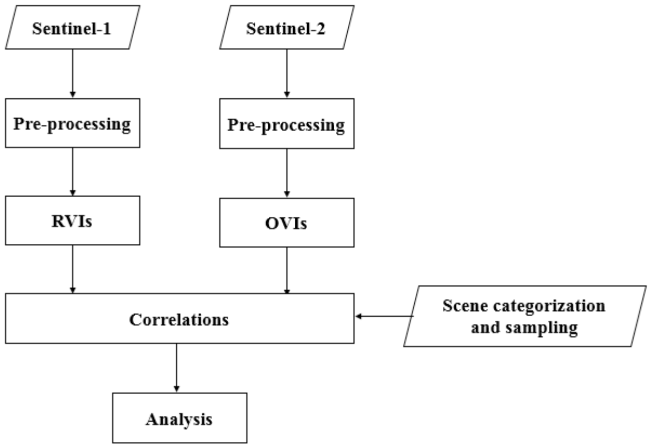

Fig. 2. Flowchart of the study.

2. **Vegetation index computation:**
   - **RVIs**: mRFDI for Sentinel-1 data is a dual-pol SAR-based index used to monitor forest structural changes, degradation, and recovery. It is calculated as the normalized difference between the backscatter coefficients of VV and VH polarizations, given by the formula (Çolak et al., 2021):

$$\boldsymbol{mRFDI} = \frac{\gamma_{vv}^{0} - \gamma_{vh}^{0}}{\gamma_{vv}^{0} + \gamma_{vh}^{0}} \ , \tag{1}$$

   The index values experimentally range from 0 to 1 (Chhabra et al., 2022), where lower values indicate undisturbed vegetated areas, while higher values represent the urban and deforested areas. This index adapts the traditional RFDI by substituting VV for HH and VH for HV, making it suitable for Sentinel-1's polarization configuration (Nicolau et al., 2021).
   mRVI is a dual-polarization adaptation of RVI, specifically designed for Sentinel-1's VV and VH backscattering data, and is calculated using the following formula (Nicolau et al., 2021):

$$\boldsymbol{mRVI} = \left(\frac{\boldsymbol{\gamma_{vv}^{0}}}{\boldsymbol{\gamma_{vv}^{0} + \gamma_{vh}^{0}}}\right)^{\mathbf{0.5}} \left(\frac{\mathbf{4}\,\boldsymbol{\gamma_{vh}^{0}}}{\boldsymbol{\gamma_{vv}^{0} + \gamma_{vh}^{0}}}\right), \tag{2}$$

   This index ranges from 0 to 1, where low values indicate smooth surfaces like bare soil or water and higher values reflect vegetational areas due to increased volume scattering from canopy complexity.
   - **OVIs:** NDVI is a widely used vegetation index that measures the health and density of vegetation based on the difference between Near-Infrared (NIR) and Red reflectance. The formula is given by (Shobairi et al., 2024):

$$\mathbf{NDVI} = \frac{(\mathrm{NIR} - \mathrm{Red})}{(\mathrm{NIR} + \mathrm{Red})}, \tag{3}$$

NIR (Sentinel-2 Band 8) reflects strongly in healthy vegetation, while Red (Sentinel-2 Band 4) is absorbed by chlorophyll. NDVI values range from −1 to 1, where negative values indicate water or built-up areas, near-zero values represent bare soil, and positive values (0.2–1) suggest increasing vegetation health and density. This index is particularly useful for monitoring plant growth, assessing drought conditions, and tracking land cover changes over time.

RVI is another vegetation index that emphasizes the ratio of NIR to Red reflectance, rather than their normalized difference. It is calculated as (Li et al., 2014):

$$\mathbf{RVI} = \frac{\mathrm{NIR}}{\mathrm{Red}}, \tag{4}$$

making it a simple yet effective measure of vegetation vigor. Unlike NDVI, RVI values are always positive, typically ranging from around 1 for barren land to higher values (above 3) for dense, healthy vegetation. RVI is particularly useful in cases where NDVI saturates in areas with very dense vegetation, and it can be beneficial for applications such as precision agriculture and remote sensing-based machine learning models.

3. **Study area categorization:**
   - In this study, to better analyze the relationships between OVIs and RVIs, we compared them in four types of groups based on visual inspection as follows:
   - **Non-vegetated areas**: Urban zones, barren lands, and waterbodies, where vegetation indices are expected to be negative and near zero
   - **Sparse vegetation**: Areas with low vegetation density, such as grasslands, farmlands, and croplands in early growth stages have positive mid-level of NDVI values.
   - **Dense vegetation:** Forested areas with high biomass and canopy cover with high NDVI values
   - **Whole scene with mixed land cover:** In this group, the whole scene from the study area is used in the analysis.
4. **Correlation analysis:**
   Pearson's correlation coefficient (r) was used to evaluate the linear relationship between **RVIs** from **Sentinel-1** and **OVIs** from **Sentinel-2**. This analysis quantifies the strength and direction of the association between radar- and optical-based vegetation metrics, which capture different aspects of vegetation structure and health. For each index pair (**RVIs vs. OVIs**), r was computed as (Cui et al., 2020):

$$\boldsymbol{r} = \frac{\sum_{i=1}^{n}(x_i-\bar{x})(y_i-\bar{y})}{\sqrt{\sum_{i=1}^{n}(x_i-\bar{x})^2}\sqrt{\sum_{i=1}^{n}(y_i-\bar{y})^2}}, \tag{5}$$

where x_i, y_i are the paired values of RVIs and OVIs for the i-th pixel, $\bar{x}$, $\bar{y}$ are the mean values of RVIs and OVIs, respectively, and n is the number of observations (pixels). The coefficient (r) ranges from **−1 to +1**, where **+1**: perfect positive linear relationship (as RVIs increase, the OVIs increase), **−1**: perfect negative linear relationship (as RVIs increase, the OVIs decrease), and **0**: no linear relationship.

In this study, we considered the following guidelines for r values:

Weak: $|r|<0.3$
Moderate: $0.3\leq|r|<0.70$
Strong: $|r|\geq0.7$

In this study, we also used the p-value to determine whether the observed Pearson correlation coefficient (r) between OVIs and RVIs is statistically significant or likely due to random chance. A p-value less than 0.05 indicates that the correlation is statistically significant, meaning there is strong evidence to reject the null hypothesis (no linear relationship) and conclude that a meaningful linear association exists (Komaroff, 2020). Conversely, a p-value greater than 0.05 suggests insufficient evidence to claim a significant linear relationship, implying the observed correlation could be random.

Experimental results

This section presents the results of our comparative analysis between Sentinel-1 vegetation indices (mRFDI, mRVI) and Sentinel-2 vegetation indices (NDVI, RVI) across different groups of land cover in Gilan province, Iran. To further investigate their relationships, we present the results in the following four subsections.

Non-vegetated areas

To calculate the correlations in non-vegetated areas, we manually selected 100 random points from non-vegetated land cover classes through visual inspection of Sentinel imagery and various spectral indices. The computed correlation coefficients along with the p-values for RVIs and OVIs are as follows:

- mRVI–mRFDI: $r = -0.99$ ($p < 0.001$),
- mRVI–NDVI: $r = -0.14$ ($p > 0.05$),
- mRFDI–NDVI: $r = 0.15$ ($p > 0.05$),
- mRVI–RVI: $r = -0.14$ ($p > 0.05$), and
- mRFDI–RVI: $r = 0.15$ ($p > 0.05$).

Correlation analysis in non-vegetated areas showed a very strong negative relationship between the radar-based indices mRVI and mRFDI ($r = -0.99$, $p < 0.001$), indicating that they capture related surface features in such environments. In contrast, all correlations between radar-based indices (mRVI, mRFDI) and optical indices (NDVI, RVI) were weak and statistically insignificant ($|r| \approx 0.14–0.15$, $p > 0.05$). This is expected, as RVIs primarily capture surface roughness and moisture, while optical indices rely on chlorophyll reflectance, which is absent in non-vegetated areas. Consequently, optical indices exhibit reduced sensitivity, whereas SAR remains responsive to physical terrain characteristics, leading to weak and statistically insignificant correlations.

Sparse vegetation

As in the previous subsection, to calculate the correlations in sparse-vegetated areas, we manually selected 100 random points from sparse-vegetated classes through visual inspection of Sentinel imagery and various spectral indices. The computed correlation coefficients and p-values are as follows:

- mRFDI–mRVI: $r = -0.99$ ($p < 0.001$),
- mRVI–NDVI: $r = 0.21$ ($p < 0.05$),
- mRFDI–NDVI: $r = -0.21$ ($p < 0.05$),

- mRVI–RVI: $r = 0.39$ ($p < 0.001$), and
- mRFDI–RVI: $r = -0.39$ ($p < 0.001$).

In sparse vegetation, RVIs (**mRFDI–mRVI**: $r = -0.99$, $p < 0.001$) retained a near-perfect inverse correlation, emphasizing their strong relationship even in limited vegetation cover. The moderate correlations between radar and RVI indices (mRVI–RVI: $r = 0.39$, mRFDI–RVI: $r = -0.39$) suggest partial alignment as vegetation density increases, reflecting radar's sensitivity to structural characteristics and RVI's responsiveness to vegetation greenness. However, since RVI is not normalized, it is more susceptible to background effects such as soil brightness, which may enhance or distort its correlation with radar signals, especially in sparsely vegetated areas. In contrast, the weaker correlation between radar and NDVI ($r = 0.21$) may result from NDVI's normalization, which not only dampens background influences but can also reduce sensitivity to subtle structural changes that radar captures. These findings highlight the different sensitivities of optical indices under varying conditions and underscore the importance of integrating radar and optical data to more accurately monitor early vegetation dynamics.

Dense vegetation

As in the previous subsection, to calculate the correlations in dense-vegetated areas, we manually selected 100 random points from dense-vegetated classes through visual inspection of Sentinel imagery and various spectral indices. The computed correlation coefficients and p-values are as follows:

- mRFDI–mRVI: $r = -0.998$ ($p < 0.001$),
- mRVI–NDVI: $r = -0.045$ ($p > 0.05$),
- mRFDI–NDVI: $r = 0.041$ ($p > 0.05$),
- mRVI–RVI: $r = -0.022$ ($p > 0.05$), and
- mRFDI–RVI: $r = 0.017$ ($p > 0.05$).

In dense vegetation, radar indices (mRFDI–mRVI: $r = -0.998$, $p < 0.001$) maintained a near-perfect inverse relationship, confirming their robust sensitivity to structural characteristics such as canopy layering, roughness, and internal moisture distribution—even in highly complex vegetative environments. In contrast, all radar–optical index combinations (mRVI–NDVI, mRFDI–NDVI, mRVI–RVI, and mRFDI–RVI) exhibited negligible and statistically insignificant correlations ($|r| < 0.05$, $p > 0.05$), indicating a near-total decoupling of radar and optical sensor responses under dense canopy conditions. This divergence is primarily due to the saturation effect in OVIs like NDVI, which plateau in dense biomass and thus lose sensitivity to further increases in chlorophyll content or leaf area index. Meanwhile, radar backscatter continues to respond to internal vegetation structure and dielectric properties—features not detectable by optical sensors. These findings underscore the fundamental difference in how radar and optical systems interact with dense vegetation and reinforce the critical importance of multi-sensor integration. By combining structural insights from radar with biochemical information from optical sensors, researchers can achieve a more comprehensive and accurate assessment of forest health, biomass dynamics, and ecological change.

Province scene with mixed landcover

In this subsection, the correlations between OVIs and RVIs are computed based on the all pixels that exist in the scene. The whole scene contains different land cover such as water, barren land, urban, agricultural, and forest areas. The computed correlation coefficients and p-values are as follows:

- mRVI–mRFDI: $r = -0.99$ ($p < 0.001$),
- mRVI–NDVI: $r = 0.42$ ($p < 0.001$),
- mRFDI–NDVI: $r = -0.39$ ($p < 0.001$),
- mRVI–RVI: $r = 0.29$ ($p < 0.001$), and
- mRFDI–RVI: $r = -0.27$ ($p < 0.001$).

In the mixed land cover scene, the results demonstrated significant variability in the relationships between RVIs and OVIs. The strong negative correlation between mRVI and mRFDI ($r = -0.99$, $p < 0.001$) emphasizes their inverse responses, with mRVI capturing the structural features of vegetation and mRFDI detecting bare soil or degraded land. Moderate positive correlations between mRVI and optical indices, such as NDVI ($r = 0.42$) and RVI ($r = 0.29$), suggest that mRVI is somewhat aligned with optical signals, particularly when we consider the whole province scene which is dominated by sparse vegetation and non-vegetation classes. However, the negative correlation between mRFDI and optical indices (NDVI: $r = -0.39$, RVI: $r = -0.27$) highlights that high mRFDI values are more closely related to non-vegetated surfaces and land degradation, where optical indices exhibit minimal response in this area. These findings underscore the complementary roles of radar and optical indices in capturing both structural and biochemical properties across diverse land cover types, reinforcing the need for combined radar–optical approaches in large-scale environmental monitoring.

Discussion

The four images illustrated in Fig. 3 show the spatial distributions of RVIs (mRVI, mRFDI) and OVIs (NDVI, RVI) over the same study area, offering insights into the vegetation structure and biochemical properties. The mRVI image shows high values in rough, vegetation-rich regions, while lower values dominate smoother surfaces like bare soil or water. Conversely, mRFDI exhibits an inverse pattern, with high values over smooth surfaces and low values over dense vegetation, reinforcing its sensitivity to terrain roughness rather than biomass presence. The NDVI image reveals a strong contrast between vegetated and non-vegetated areas, effectively capturing the chlorophyll content, while RVI, another optical index, appears to follow a similar pattern but with slightly different intensity variations. On comparing RVIs and OVIs, areas with dense vegetation in NDVI and RVI generally align with mid to high mRVI and mid to low mRFDI, confirming the structural and biochemical relationship of vegetation. However, local-scale discrepancies observed in the correlation analysis emphasize the need for careful interpretation. It is important to note that these results are influenced by factors such as cloud cover, sampling strategy, seasonal variations, and the underlying land cover, which can affect sensor performance and data interpretation. This highlights the complementary nature of radar and optical indices in remote sensing-based vegetation analysis, where integrating both sources provides a more comprehensive understanding of ecosystem characteristics.

The near-perfect inverse correlation between RVIs (mRVI–mRFDI: $r \approx -0.99$) highlights their shared sensitivity to structural properties such as canopy roughness and moisture content. In contrast, their weak-to-moderate correlations with OVIs ($|r|$

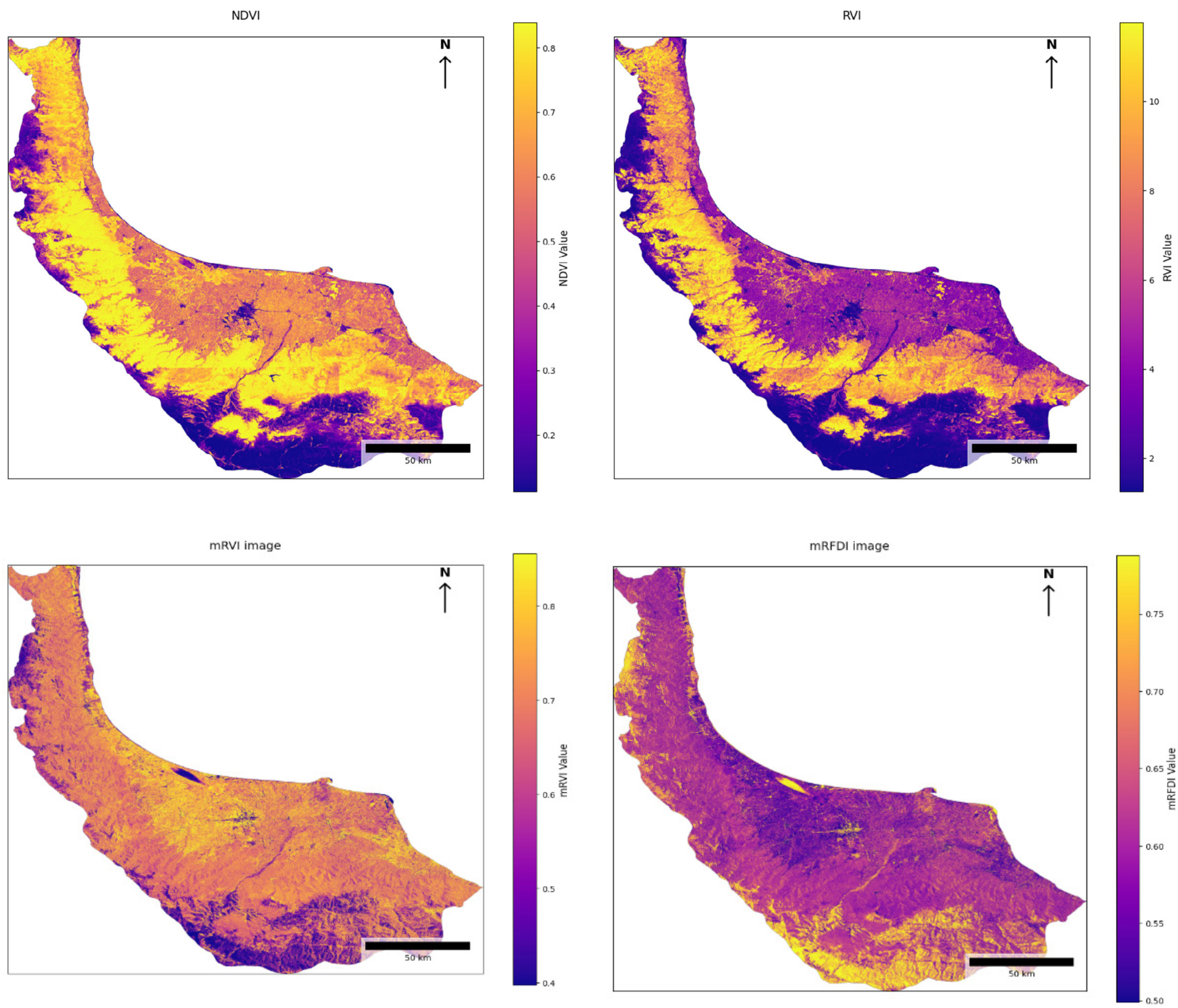

Fig. 3. Outputs of the vegetation indices for Gilan province.

< 0.4) point to fundamental differences in how radar and optical data capture vegetation characteristics: radar is more responsive to physical structure (e.g., surface roughness, biomass, moisture), while optical indices like NDVI primarily reflect biochemical properties (e.g., chlorophyll content). This complementarity is particularly important in scenarios where optical data may be limited, as radar may penetrate dense canopies and is less affected by saturation, such as in very dense vegetation, providing insight into structural and moisture dynamics that optical sensors cannot detect. However, optical indices excel in tracking photosynthetic activity, filling in where radar signals saturate or lose sensitivity in complex canopies. The experimental results reveal significant landcover dependencies in index relationships. In all situations, radar-based indices (mRVI and mRFDI) show a near-perfect inverse correlation ($r = -0.998$, $p < 0.001$), underscoring their consistent sensitivity to structural properties such as canopy roughness, moisture, and biomass arrangement. However, the negligible correlations between RVIs and OVIs (NDVI and RVI, $|r| < 0.05$, $p > 0.05$) in dense vegetation areas highlight a complete decoupling of sensor responses—optical indices saturate in dense canopies and lose sensitivity to incremental changes in chlorophyll, while radar sensors continue to capture underlying physical characteristics. Conversely, in mixed landscapes, where diverse land cover types such as water, barren land, urban, agricultural, and forest areas coexist, moderate correlations between mRVI and optical indices (NDVI: $r = 0.42$, RVI: $r = 0.29$) emerge, highlighting the role of existing mixed landcover pixels in calculating the correlation.

These findings have important operational implications. Monitoring systems should leverage both radar and optical data to overcome the limitations of each sensor type. For instance, radar is particularly useful when cloud cover obscures optical imagery or when capturing structural vegetation properties is essential. In homogeneous landscapes, an integrated fusion of radar–optical data may be necessary to bridge the gap between physical structure and biochemical properties, while in mixed landscapes, the inherent sensor synergy reduces the need for resource-intensive fusion.

Future research should aim to validate these patterns across different biomes and phenological stages, explore advanced sensor fusion techniques, and develop land cover-specific interpretation methods. Investigating potential nonlinear relationships between sensors may further improve the accuracy and efficiency of vegetation monitoring systems.

Conclusion

This study conducted in Gilan province, Iran, reveals that radar (mRVI, mRFDI) and optical (NDVI, RVI) vegetation indices exhibit landcover-dependent relationships. Radar indices show near-perfect inverse correlations (mRVI–mRFDI: $r \approx -0.99$) across all environments, confirming structural reliability. Radar–optical correlations vary: they are negligible in non-vegetated ($|r| < 0.15$) and dense-vegetated ($|r| < 0.05$) areas due to optical limitations (saturation or absent chlorophyll), but are moderate in mixed landscapes (e.g., mRVI–NDVI: $r = 0.42$) where structural and biochemical signals partially align. Sparse vegetation shows transitional ties (e.g., mRVI–RVI: $r = 0.39$), highlighting early sensor synergy. Radar excels in cloud-prone regions and structural monitoring (degradation, soil moisture), while optical tracks chlorophyll dynamics. Future work should investigate whether these patterns hold across different climatic regions and vegetation types and how they scale with different resolution choices.

References

Çolak, E., Chandra, M. & Sunar F. (2021).The use of sentinel 1/2 vegetation indexes with gee time series data in detecting land cover changes in the sinop nuclear power plant construction site. *The International Archives of the Photogrammetry, Remote Sensing and Spatial Information Sciences,* 43, 701-706. DOI: 10.5194/isprs-archives-XLIII-B3-2021-701-2021.

Cui, W., Sun, Z., Ma, H. & Wu S. (2020). The correlation analysis of atmospheric model accuracy based on the pearson correlation criterion. *IOP Conference Series: Materials Science and Engineering,* 780 (3), 032045. DOI: 10.1088/1757-899X/780/3/032045.

De La Iglesia Martinez, A. & Labib S. (2023). Demystifying normalized difference vegetation index (NDVI) for greenness exposure assessments and policy interventions in urban greening. *Environ. Res.,* 220, 115155. DOI: 10.1016/j.envres.2022.115155.

Gonenc, A. & Ozerdem M.S. (2019). Comparison of NDVI and RVI vegetation indices using satellite images. In *2019 8th International Conference on Agro-Geoinformatics (Agro-Geoinformatics)* (pp. 1-4). IEEE. DOI: 10.1109/Agro-Geoinformatics.2019.8820225.

Gupta, R. (1993). Comparative study of AVHRR ratio vegetation index and normalized difference vegetation index in district level agricultural monitoring. *Int. J. Remote Sens.,* 14(1), 53-73. DOI: 10.1080/01431169308904321.

Hu, X., Li, L., Huang, J., Zeng, Y., Zhang, S., Su, Y., Hong, Y. & Hong Z. (2024). Radar vegetation indices for monitoring surface vegetation: Developments, challenges, and trends. *Sci. Total Environ.,* 945, 173974. DOI: 10.1016/j.scitotenv.2024.173974.

Chhabra, A., Rüdiger, C., Yebra, M., Jagdhuber, T. & Hilton J. (2022). RADAR-vegetation structural perpendicular index (R-VSPI) for the quantification of wildfire impact and post-fire vegetation recovery. *Remote Sensing,* 14(13), 3132. DOI: 10.3390/rs14133132.

Kim, Y.-H., Oh, J.-H. & Kim Y.-I. (2014). Comparative analysis of the multispectral vegetation indices and the radar vegetation index. *Journal of the Korean Society of Surveying, Geodesy, Photogrammetry and Cartography,* 32(6), 607-615. DOI: 10.7848/ksgpc.2014.32.6.607.

Komaroff, E. (2020). Relationships between p-values and Pearson correlation coefficients, type 1 errors and effect size errors, under a true null hypothesis. *Journal of Statistical Theory and Practice,* 14(3), 49. DOI: 10.1007/s42519-020-00115-6.

Li, F., Miao, Y., Feng, G., Yuan, F., Yue, S., Gao, X., Liu, Y., Liu, B., Ustin, S.L. & Chen X. (2014). Improving estimation of summer maize nitrogen status with red edge-based spectral vegetation indices. *Field Crops Res.,* 157, 111-123. DOI: 10.1016/j.fcr.2013.12.018.

Nicolau, A.P., Flores-Anderson, A., Griffin, R., Herndon, K. & Meyer F.J. (2021). Assessing SAR C-band data to effectively distinguish modified land uses in a heavily disturbed Amazon forest. *International Journal of Applied Earth Observation and Geoinformation,* 94, 102214. DOI: 10.1016/j.jag.2020.102214.

Shao, Y., Hu, Q., Guo, H., Lu, Y., Dong, Q. & Han C. (2003). Effect of dielectric properties of moist salinized soils on backscattering coefficients extracted from RADARSAT image. *IEEE Transactions on Geoscience and Remote Sensing,* 41(8), 8, 1879-1888. DOI: 10.1109/TGRS.2003.813499.

Shobairi, S.O.R., Lingxiao, S., Haiyan, Z., Chunlan, L., Jing, H. & Beirami B.A. (2024). Monitoring the temporal-spatial changes of vegetation cover and drivers in Tian Shan ecoregions, China. *Folia Forestalia Polonica, Ser. A. Forestry,* 66(3), 155-182. DOI: 10.2478/ffp-2024-0013.

Spadoni, G.L., Cavalli, A., Congedo, L. & Munafò M. (2020). Analysis of Normalized Difference Vegetation Index (NDVI) multi-temporal series for the production of forest cartography. *Remote Sensing Applications: Society and Environment,* 20, 100419. DOI: 10.1016/j.rsase.2020.100419.

Tsokas, A., Rysz, M., Pardalos, P.M. & Dipple K. (2022). SAR data applications in earth observation: An Overview. *Expert Systems with Applications,* 205, 117342. DOI: 10.1016/j.eswa.2022.117342.

Wu, G., Zhou, Z., Zhao, X., Huang, D., Long, Y. & Peng R. (2025). Study on correlation between crop optical vegetation index and radar parameters and its influencing factors based on plot unit. *Geocarto International,* 40(1), 2453621. DOI: 10.1080/10106049.2025.2453621.

Xue, J. & Su B. (2017). Significant remote sensing vegetation indices: A review of developments and Applications. *Journal of Sensors,* 2017(1), 1353691. DOI: 10.1155/2017/1353691.

Zhou, Y., Flynn K.C., Gowda, P.H., Wagle, P., Ma, S., Kakani, V.G. & Steiner J.L. (2021). The potential of active and passive remote sensing to detect frequent harvesting of alfalfa. *International Journal of Applied Earth Observation and Geoinformation,* 104, 102539. DOI: 10.1016/j.jag.2021.102539.